JOURNAL OF AGRICULTURAL AND FOOD CHEMISTRY

J. Agric. Food Chem. **2002,** *50,* 1593−1601 **1593**

Polyphenol/Peptide Binding and Precipitation

ADRIAN J. CHARLTON,[†,‡] NICOLA J. BAXTER,[†] M. LOKMAN KHAN,[§,#] ARTHUR J. G. MOIR,[†] EDWIN HASLAM,[§] ALAN P. DAVIES,[⊥] AND MICHAEL P. WILLIAMSON*[,†]

Department of Molecular Biology and Biotechnology and Department of Chemistry, University of Sheffield, Sheffield S10 2TN, United Kingdom, and Unilever Research, Colworth House, Sharnbrook, Bedford MK44 1LQ, United Kingdom

Polyphenols are largely responsible for the astringency and "mouthfeel" of tea and wine by their interactions with basic salivary proline-rich proteins. Astringency arises from precipitation of polyphenol/peptide complexes, which is an important protective mechanism in animals that consume polyphenols. This paper presents biophysical studies of the interactions between chemically defined polyphenols and peptides. It is shown that intermolecular binding is dominated by stacking of polyphenolic rings onto planar hydrophobic surfaces and is strengthened by multiple cooperative binding of polyphenolic rings. Affinities weaken at higher temperatures and are unaffected by pH between pH 3.8 and 6.0. Measurements of self-diffusion rates for peptides with increasing concentrations of polyphenol demonstrate that peptides become increasingly coated with polyphenol. When the coating is sufficiently extensive to provide cooperative polyphenol bridges, the peptide dimerizes and precipitates. Light scattering measurements and electron microscopy indicate that the insoluble particles fall into two discrete size classes of ca. 80 and 500 nm diameter. The larger particles are favored at higher temperature and pH, suggesting that the particles are in a colloidal state, with the smaller particles being stabilized by charge repulsion between particles, and that precipitation of the complexes may be a phase separation process.

KEYWORDS: Polyphenol; tannin; salivary protein; NMR; diffusion; light scattering

INTRODUCTION

Polyphenols, also known as vegetable tannins, are found in a wide variety of foodstuffs and beverages, being particularly highly concentrated in green and black teas, wine (especially red wine), some fruits, and cereals such as millet and sorghum. They have been classified into two major groups: the condensed polyphenols, based on a flavonoid framework, and the hydrolyzable polyphenols, which are essentially galloyl esters of glucose (**Figure 1**) (*1*). They are frequently associated with a bitter taste, but they also give rise to the oral sensation of astringency (*2*). Astringency is a puckering or drying sensation, not localized to any one part of the mouth, and typically both develops and dissipates slowly. This study is part of ongoing research to understand the molecular basis of astringency, which is clearly rooted in the interactions between polyphenols and other species naturally present in the oral cavity and, in particular, the basic salivary proline-rich proteins (*3*).

The salivary proline-rich proteins constitute 70% of the proteins in saliva and are made up of three types: the acidic, glycosylated, and basic proteins, which comprise roughly 30, 23, and 17% of unstimulated saliva, respectively (*4*). Acidic and glycosylated proline-rich proteins have functions, respectively, to control calcium levels and to aid lubrication of food boluses (*5*−*7*), but the only known biological function of the basic proteins is to bind to polyphenols (*8*). Basic proline-rich proteins have a similar sequence across a wide range of species. Typically they comprise an ∼19-residue sequence that is dominated by proline, glutamine, and glycine, which is repeated with variations between 5 and 15 times to give a protein of roughly 150 amino acids in length (*9*), which is typically extended in solution (*10*).

It has been shown that polyphenols can have a variety of harmful effects on animals, including sequestration of dietary iron and inhibition of digestive enzymes, and that salivary proline-rich proteins can bind to the polyphenols and precipitate them, thereby effectively preventing them from becoming bioavailable and having any effect in the gastrointestinal tract (*11*−*13*). This function of the proline-rich proteins is supported by a large number of studies; in particular, studies that show that basic salivary proline-rich proteins are produced only by

* Author to whom correspondence should be addressed (fax +44 114 272 8697; telephone +44 114 222 4224; e-mail M.Williamson@Sheffield.ac.uk).
[†] Department of Molecular Biology and Biotechnology.
[‡] Present address: Central Science Laboratory, Sand Hutton, York YO41 1LZ, U.K.
[§] Department of Chemistry.
[#] Present address: School of Agricultural and Forest Sciences, University of Wales, Bangor, LL57 2UW, U.K.
[⊥] Unilever Research.

10.1021/jf010897z CCC: $22.00
Published on Web 02/12/2002

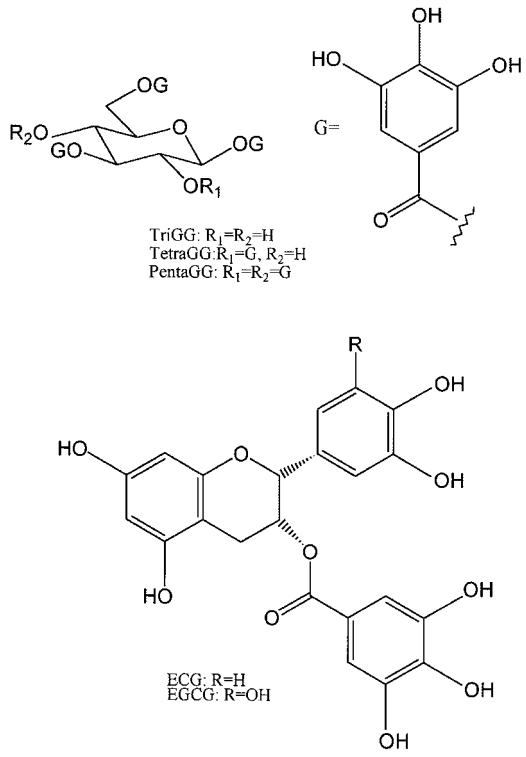

Figure 1. Structures of typical hydrolyzable polyphenols (galloylglucoses) and condensed polyphenols [epigallocatechin gallate (EGCG) and epicatechin gallate (ECG)]. Propyl gallate is the propyl ester of gallic acid (top right).

animals that consume significant quantities of polyphenol in the diet (*14*). It therefore seems likely that the astringent sensation is a consequence of interactions between basic proline-rich proteins and polyphenols. Most studies in this area have been hampered by the complexity of the in vivo situation and by the subjective nature of the observations made, which make it difficult to identify or quantify the molecular components responsible for any observed effect. We have therefore used a range of pure proteins and polyphenols and carried out detailed measurements on the systems. The results allow us for the first time to propose a detailed molecular description of the processes occurring, which may be relevant to other protein precipitation events such as those occurring during amyloidosis.

MATERIALS AND METHODS

Materials. Epigallocatechin gallate (EGCG) and epicatechin gallate (ECG) were gifts from Unilever Research, Colworth, U.K., and were purified from green tea extract. Pentagalloylglucose (PGG) was prepared from tannic acid (*15*), trigalloylglucose from myrabolans (*Terminalia chebula*) (*16*), and tetragalloylglucose from Turkish oak galls (*15*, *17*). Propyl gallate was a gift from Dr. Mike Saltmarsh, Foursquare Ltd., U.K. Bradykinin (1060 Da) was purchased from Sigma Chemical Co. The N-terminal region of the mouse salivary acidic proline-rich protein MP5 (ref *18*; 2700 Da) and the 7-mer and 19-mer basic proline-rich peptides (740 and 2000 Da, respectively) were synthesized using a Milligen 9050 peptide synthesizer with FMOC chemistry and purified using HPLC on a C_{18} column. The sequences are listed in **Table 1**.

The histatins were purified from human saliva using the method of Levine and Keller (*19*) with modifications described in subsequent papers from the Keller group (*4*, *20*−*22*). Briefly, parotid saliva was collected using a suction cup (*23*), and ethylenediaminetetraacetate (EDTA) was added to a final concentration of 5 mM. Globular proteins were removed using a 45% ammonium sulfate cut followed by extensive dialysis against water. A lyophilized and redissolved sample was applied to a DEAE-Sephadex A-25 column (100 × 2.5 cm) and eluted using 5 mM Tris buffer, pH 8.6. The run-through was lyophilized and applied to a Sephadex G-150 column (100 × 2.5 cm), eluted with the same buffer. Protein eluted in three broad peaks, of which the third peak constituted a mixture of histatins, as described in ref *24*. From SDS-PAGE gels, the histatins had molecular weights of between 1 and 6 kDa.

Polyphenol Self-Association. Polyphenol self-association was analyzed using the isodesmic model (*25*), which assumes that polyphenols associate to form stacks, where the self-association constant K_a is the same for each association step

$$\Delta\delta_i = \Delta\delta_{max} K_a [T]_0 \{2/[1 + (4K_a[T]_0 + 1)^{1/2}]\}^2 \quad (1)$$

where $\Delta\delta_i$ is the change in chemical shift of a polyphenol signal, $\Delta\delta_{max}$ is the maximum shift, and $[T]_0$ is the total concentration of polyphenols. Solutions of polyphenol (typically 20 mM) were diluted sequentially to ∼0.1 mM; at each dilution NMR spectra were acquired, and the chemical shifts of several signals were measured. Equation 1 was fitted to the measured shifts using a least-squares method to calculate a mean value of K_a, as described in ref *26*.

Peptide/Polyphenol Binding Affinity. From a consideration of binding equilibria at *n* multiple equivalent sites, the concentration of peptide bound by polyphenol is given by

$$[PT] = \{(K_d + n[P]_i + [T]_i) \pm [(K_d + n[P]_i + [T]_i)^2 - 4n[P]_i[T]_i]^{1/2}\}/2n \quad (2)$$

whence the dissociation constant K_d is obtained using the equation

$$\Delta\delta_i = \frac{\Delta\delta_{max}}{2}\left\{\left(1 + \frac{K_d}{n[P]_i} + \frac{[T]_i}{n[P]_i}\right) - \left(\left[1 + \frac{K_d}{n[P]_i} + \frac{[T]_i}{n[P]_i}\right]^2 - \frac{4[T]_i}{n[P]_i}\right)^{1/2}\right\} \quad (3)$$

where $[P]_i$ is the total peptide concentration and $[T]_i$ is the concentration of self-associated polyphenol species. $[T]_i$ can be related to $[T]_0$ using the equations (*26*)

$$[T]_i = [T]/(1 - K_a[T]) \quad (4)$$

and

$$[T] = [T]_0\{2/[1 + (4K_a[T]_0 + 1)^{1/2}]\}^2 \quad (5)$$

where [T] is the concentration of polyphenol monomer. The concentration of any given aggregated species can then be calculated using the equilibrium constant:

$$[T_n] = K_a^{n-1}[T]^n \quad (6)$$

Polyphenol solutions (∼20 mM, depending on the solubility of the polyphenol) were titrated into a solution of peptide (2 mM) in a range of different solution conditions as listed in **Table 2**, and NMR spectra were acquired at each titration point. Chemical shifts of individual assigned resonances were measured. Each resonance was fitted separately to eq 3. Trial values of K_d were kept fixed, and χ^2 values were calculated for the best fit by allowing *n* and $\Delta\delta_{max}$ to vary independently for each proton. The mean values of K_d and *n* from taking the minimum χ^2 values from fits of individual protons were calculated and used to generate estimates for the error. Further details of the fitting are given in ref *26* and in the text.

Diffusion Experiments. A solution of polyphenol (∼20 mM) was titrated into the peptide (2 mM) at 3 °C. A set of 10 pulsed field gradient spin−echo experiments (*27*) was carried out at each step of the titration, with the maximum strength of the 8 ms sine-shaped gradient pulses increasing in 5 G cm^{-1} steps from 0 to 45 G cm^{-1} and a 12 ms diffusion period. The intensity of several peptide resonances was measured using an integration routine in FELIX (Molecular Simulation, Inc.), and the diffusion constant was obtained from the slope of the graph of log-

Table 1. Chemical Shift Changes and Precipitation Observed on Titrating Polyphenols into Proteins

protein/polyphenol	protein sequence	observations on titration
acidic PRP + propyl gallate	QRVDEGISYRGDNSSRGHSTTVVSD	all shift changes small: largest are to R2, Y9, R10, R16, and H18; no precipitation
histatin + EGCG	typical sequence ...HAKRHHGYKRKFHEKHHSHR...	very small changes (<0.07 ppm); no precipitation
bradykinin + EGCG	RPPGFSPFR	largest shift changes F8 ∼ F5 ∼ P2 > P7 ≫ P3; all changes within Phe are in the aromatic ring; precipitates
bradykinin + polygalloylglucoses	RPPGFSPFR	shift changes and precipitation in the order pentaGG > tetraGG ≫ triGG
7-mer basic PRP repeat sequence + EGCG	QGRPPQG	largest changes in P4 and P5; very small change to G, Q; little precipitation
19-mer basic PRP repeat sequence + EGCG, ECG or PGG	QGPPPQGGPQQRPPQPPNQ	shift changes and precipitation PGG > EGCG ≈ ECG; precipitation least at high temperature and low pH; largest shift changes P3 ≈ P4 >P13 ≈ P16 > P5 ≈ P14 ≈ P17 > R12; essentially zero change to G, Q, and N

Table 2. Binding Affinities between Polyphenols and Proteins

row	peptide/polyphenol[a]	conditions	K_a for polyphenol[b]	K_d (mean ± SD) (mM)	n[c] (mean ± SD)
1	bradykinin/PGG	20% DMSO, pH 5.9, 22 °C	0.025 ± 0.005	500[d]	5 ± 0.6
2	ΔR^1-bradykinin/PGG[e]	20% DMSO, pH 5.9, 22 °C	0.025 ± 0.005	500[d]	5 ± 1
3	ΔR^9-bradykinin/PGG[e]	20% DMSO, pH 5.9, 22 °C	0.025 ± 0.005	300[d]	5 ± 0.4
4	7-mer/EGCG	10% DMSO, pH 3.8, 27 °C	0.018 ± 0.005	360 ± 180	1.2 ± 0.5
5	19-mer/EGCG	10% DMSO, pH 3.8, 3 °C	0.049 ± 0.010	2.4 ± 2.2	3.1 ± 1.2
6	19-mer/EGCG	10% DMSO, pH 3.8, 27 °C	0.018 ± 0.005	7.8 ± 3.8	7.6 ± 1.3
7	19-mer/EGCG	10% DMSO, pH 3.8, 55 °C	0.004 ± 0.0008	33 ± 12	7.5
8	19-mer/EGCG	10% DMSO, pH 4.8, 27 °C	0.021 ± 0.0096	9.8 ± 0.9	7.5 ± 1.2
9	19-mer/EGCG	10% DMSO, pH 6.0, 27 °C	0.014 ± 0.007	6.6 ± 5.2	5.0 ± 1.9
10	19-mer/PGG	10% DMSO, pH 3.8, 3 °C[f]	0.24 ± 0.06	0.05 ± 0.02	2.2 ± 0.7
11	19-mer/PGG	10% DMSO, pH 3.8, 27 °C	0.22 ± 0.07	1.3 ± 0.6	2.0 ± 0.2

[a] See **Table 1** for details of peptide sequences. [b] Self-association constant for polyphenol (mM^{-1}). [c] Number of binding sites on the peptide for polyphenol. Fitted by assuming all binding sites have equal affinity. [d] K_d values are imprecise: estimated error is ×2 in either direction. [e] ΔR^1-bradykinin is bradykinin lacking the N-terminal arginine; ΔR^9-bradykinin lacks the C-terminal arginine. Note that because the bradykinin titrations were carried out in 20% DMSO for solubility reasons, the absolute values of K_d are weaker than they would be in 10% DMSO [f] Results taken from ref *26*.

(peak integral) versus (gradient strength)^2. For reproducible results in the presence of precipitation, it was necessary to adopt a standardized timing: for each addition of polyphenol, the sample was removed from the spectrometer for 2 min; the sample was placed back in the spectrometer and allowed to equilibrate for 15 min, after which time acquisition of the data was started. Each set of diffusion experiments took 30 min, after which the next addition of polyphenol was made. The pH values of the polyphenol and peptide solutions were carefully adjusted to pH 3.8 at the start of the experiment.

Dynamic Laser Light Scattering. Light scattering measurements were performed using an ALV-3000 (Langen, Germany) equipped with a Spectra Physics series 2000 high-power krypton ion red laser (wavelength = 647.1 nm). Measurements were taken at angles of 60−90°, and the aperture was set to give a count of between 100 and 1000. All samples were prepared 24 h before measurement and typically contained 0.17 mM 19-mer proline-rich peptide plus EGCG at a range of concentrations, in water. The pH was adjusted after the solutions had been prepared. Samples were stored at ambient temperature overnight. After the sample had ben put in the chamber, it was equilibrated at the desired temperature for 30 min before measurement. Data were collected three times for each sample. Corrections for changes in the refractive index of water with temperature were made using the parameters of ref *28*. The scattering results were analyzed by the contin routine, using Malvern PCS 1.32a software.

Electron Microscopy. Electron microscopy was carried out using a Phillips CM10 transmission electron microscope at an accelerating voltage of 80 kV. Samples were made up in water at ambient temperature and allowed to equilibrate for 24 h, after which time a drop of each sample was placed onto a 3.05 mm, 200 hexagonal mesh copper grid that had previously been coated with 1% pioloform in chloroform. The sample was allowed to air-dry for 20−30 s, after which time it was blotted dry with filter paper, and stained by adding a drop of 1% phosphotungstic acid, pH 7.2, to the grid.

Other Methods. Sequence-specific NMR resonance assignments were carried out using the sequential assignment method (*29*). The assignment of the N-terminal acidic peptide is described in ref *30*, that of bradykinin in ref *31*; and that of the 19-mer is based on ref *26* and described in ref *32*, as is that of the 7-mer. A list of assignments of the N-terminal acidic peptide is given in the Supporting Information. Assignments for ECG and EGCG were obtained from ref *33* and those for PGG from ref *30*. Measurements of the pK_a of EGCG were made using an Autotitration RTS8822 Recording Titration System (Radiometer). The titration was carried out by adding 25 mM KOH to an acidified EGCG solution; titrating in the opposite direction resulted in irreversible oxidation of EGCG at high pH.

RESULTS

Amino Acid Preference of Polyphenols. Early studies of polyphenol/protein binding suggested that polyphenols bound preferentially to proline residues (*8*). This was borne out by our previous studies, which demonstrated the key role of proline residues and, in addition, showed that NMR chemical shift changes were a good measure of binding affinity at different sites, because of the ring-current shifts caused by the aromatic polyphenol rings (*24*, *26*, *34*). However, proline is certainly not the only possible binding site. For example, it has been suggested that polyphenols bind tightly to histatins, which are salivary proteins containing a high proportion of histidine residues (*35*, *36*). We have therefore carried out a series of studies in which pure polyphenols [mainly EGCG or β-1,2,3,4,6-

penta-*O*-galloyl-D-glucopyranose (PGG), **Figure 1**] were titrated into solutions of peptides or proteins and chemical shift changes were measured. We wished to use a range of amino acid types and a range of proteins of possible physiological importance. We therefore looked at interactions with the following proteins: The N-terminal sequence of an acidic proline-rich protein, which is not itself proline-rich and contains a number of acidic residues; a partially purified histatin preparation, consisting of a mixture of several histidine-rich salivary proteins of very similar sequence and composition; bradykinin, a potent vasodilator present in blood and containing proline, arginine, and phenylalanine residues, plus two bradykinin derivatives; and both short and long versions of the basic proline-rich protein repeat sequence (a 7-mer and a 19-mer). The results are summarized in **Table 1** and show that proline is an important binding site but that interactions also occur with arginine and phenylalanine side chains. These conclusions are supported by nuclear Overhauser effect (NOE) measurements, which show close contact between polyphenolic rings and predominantly proline residues (*26*). Interestingly, chemical shift changes with histatins were very small. Similar observations have been made by Bennick, who nevertheless reported significant binding to histatins (*35*−*37*). It may be that simple chemical shift changes are not a good measure of affinity, and we therefore carried out a more detailed measurement of binding affinities to several of these proteins.

Measurements of Polyphenol/Protein Site-Specific Binding Affinity. By fitting chemical shift changes of individually assigned resonances to theoretical binding curves, it is possible to calculate binding affinities at individual sites in the peptide. The methodology is described in detail in ref *26* and is not repeated here in detail. The results of the fitting are illustrated in **Figure 2** and summarized in **Table 2**. However, before the results are discussed, there are several details of the fitting procedure that require comment.

First, because the polyphenols self-associate (via their aromatic rings, in a fashion similar to the peptide binding), the concentration of available polyphenol binding sites is less than that calculated from the total concentration of polyphenol in the solution. It is therefore necessary to measure the degree of self-association of each polyphenol under the experimental conditions before the peptide affinity can be measured. This is done by measuring the concentration dependence of polyphenol chemical shifts. Results are summarized in **Table 2**. It can be seen from **Table 2** that self-association is very significant at the concentrations used in this study, particularly for PGG, which has the strongest self-association. Self-association measurements on ECG and EGCG show that they have almost identical self-association constants (for example, at pH 3.8 and 3 °C, ECG and EGCG have self-association constants in 10% DMSO of 0.048 ± 0.019 and 0.049 ± 0.010 mM^{-1}, respectively), suggesting that the additional phenolic hydroxyl group of EGCG is not important in the self-association, in agreement with our previous results, which suggested that self-association is largely hydrophobically driven (*26*).

Second, because for solubility reasons it is not possible to carry out the titrations to saturation, it is important to conduct the curve fitting in a particularly rigorous manner. The variables to be fitted are the maximum chemical shift change of the resonance being measured, the dissociation constant at that site, and *n*, which is the total number of equivalent binding sites on the peptide for the polyphenol. In our previous study (*26*), we showed that the value of *n* is not critical and is largely predictable from the structure of the peptide and the polyphenol,

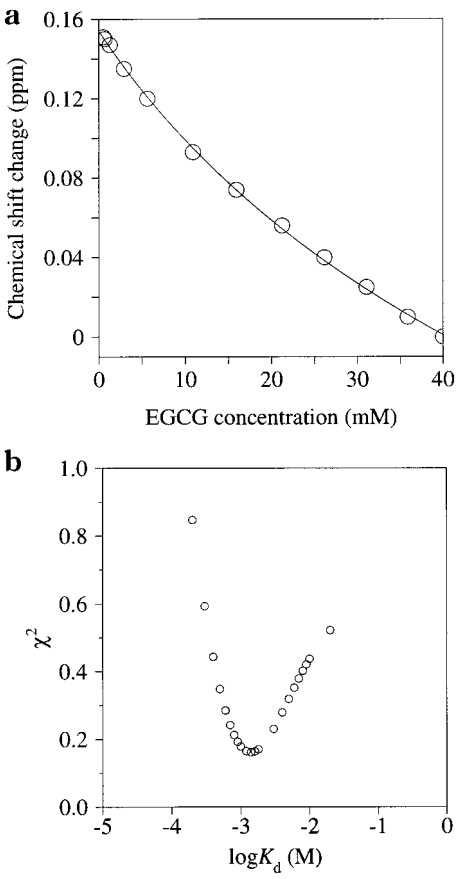

Figure 2. Results of the fitting of the dissociation constant for the binding of EGCG to the 19-mer PRP repeat (3 °C, pH 3.8): (a) chemical shift changes of EGCG H-2 with EGCG concentration, used to calculate a self-association constant (line shows the best-fit value of K_a); (b) χ^2 values for different trial values of the dissociation constant K_d, for binding of EGCG to Pro5 H^δ (optimum value of K_d is at the minimum of the curve).

being the number of polyphenols that can be simultaneously bound to the peptide. In particular, we showed that small polyphenols have a value of *n* which is similar to the combined number of (proline + arginine) residues in the sequence, implying that a binding site approximates to an amino acid. Larger polyphenols have a smaller value of *n* for a given protein sequence, because they occupy more binding sites. A similar result was obtained in the present work, which is most obviously seen by comparing the results of EGCG and PGG binding to the 19-mer peptide (**Table 2**, rows 6 and 11). EGCG can bind simultaneously at up to ∼7.5 sites (consistent with the 8 prolines present in the sequence), whereas the larger and multidentate PGG binds at only ∼2. Best results are obtained by fixing the dissociation constant K_d at different trial values and calculating the χ^2 values for the fitting using different values of K_d, as described in ref *26*. In the case of a peptide with multiple possible binding sites, to obtain binding affinities, it is necessary to make some assumptions about the binding. Trials were carried out allowing different amino acids to have different affinities, but the experimental data are not detailed enough to distinguish the different models. Therefore, in all of the results reported here, it is assumed that all binding sites have equivalent affinity.

There are several notable conclusions that can be made from the results (**Tables 1** and **2**). It is clear that proline is an important binding site, as is phenylalanine. It should, however, be noted that in most proteins, phenylalanine side chains are buried and therefore are not in general available as binding sites.

Arginine is less important (cf. the small changes in removing terminal arginines from bradykinin in **Table 2**), although it clearly contributes to binding (**Table 1**). Our previous results (*26*) showed that many polyphenols bind at multiple sites on peptides. In the current study, this can be seen, for example, from the fitted values of *n*, which show that the number of actual binding sites is significantly less than the potential total number of binding sites, given by the number of (prolines + arginines). For EGCG, most potential binding sites can be filled simultaneously, whereas for the larger and more flexible polyphenol PGG, only roughly one-fourth of the number of potential binding sites can be filled simultaneously. Therefore, the observation that arginine and proline both show chemical shift changes is at least partly due to the fact that binding at these two residues is not independent. We therefore conclude that arginine can strengthen the interaction between polyphenol and peptide by forming an additional site of interaction but does not in itself form an independent strong binding site.

The affinity of EGCG for the 7-mer peptide is ~50 times weaker than for the 19-mer of similar sequence and composition. The most significant difference between these peptides is their length and, consequently, the number of potential binding sites: the 7-mer has only one or two potential binding sites, whereas the 19-mer has approximately seven or eight. This provides strong evidence that cooperativity of polyphenol binding is important for a strong interaction and suggests that the longer peptides are able to "wrap around" polyphenols to interact at several places at once (*24*). This conclusion is supported by the marked decrease in *n* at low temperature (**Table 2**, rows 5 and 6), suggesting a more multidentate binding mode at low temperatures. As noted by a referee, the existence of cooperativity in binding invalidates the assumption of independent binding inherent to eq 2 and therefore implies that the measured dissociation constants may be in error. We justify our continued use of eq 2 (a) by the observation that the cooperativity seen is relatively weak and (b) by the fact that inclusion of cooperativity terms into the fitted equations would make them so complex that it would be very hard to know whether the results obtained were meaningful. It is, however, clear that the dissociation constants have a large associated error and are model-dependent.

As might be expected, the affinities become weaker as the temperature is increased but do not change significantly over the pH range tested. This is an interesting observation because visible precipitation of the complex is less significant at lower pH (**Table 1**) and suggests that the relationship between binding and visible precipitation is not straightforward.

Self-Diffusion Constants. It is possible to measure the self-diffusion rate of a molecule in solution using pulsed-field gradient NMR techniques. The diffusion rate is related to the radius of the molecule and therefore provides a measure of effective molecular size. Diffusion rates were measured for the 19-mer peptide in the presence of increasing concentrations of EGCG or PGG. Measurements were made up to and beyond the observation of precipitation of the polyphenol/peptide complex in the NMR tube. The precipitate forms in a time-dependent manner, and therefore for reproducible results it was necessary to follow a strict timing protocol, as described under Materials and Methods. The results are shown in **Figure 3** and demonstrate a steady decrease in diffusion rate up to approximately the point at which precipitation starts, after which the decrease in diffusion rate becomes much less rapid.

Electron Microscopy. The measurements described above enable us to characterize the binding as far as the point where the complex becomes insoluble but do not allow us to say much beyond this, because solution-state NMR is unable to give information on insoluble material. We therefore turned to other techniques to characterize the precipitates formed, namely, electron microscopy and dynamic laser light scattering.

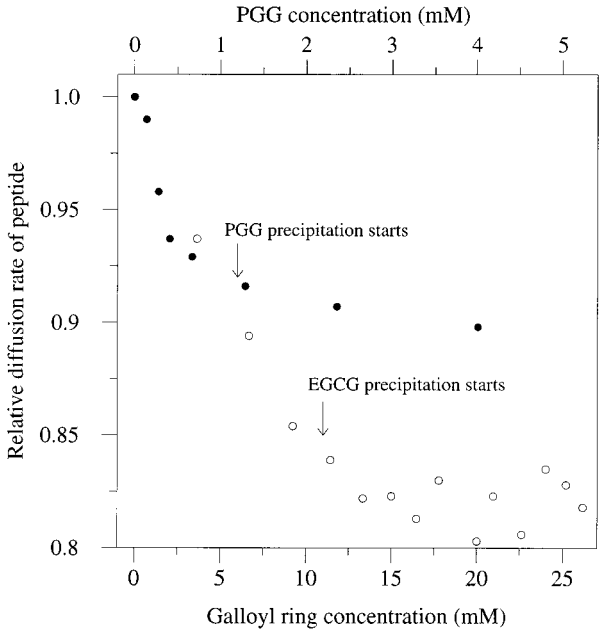

Figure 3. Self-diffusion rate for the 19-mer PRP repeat in the presence of increasing concentrations of EGCG (open circles) or PGG (solid circles), 3 °C, pH 3.8, relative to peptide in the absence of polyphenol. The results are plotted against the concentration of galloyl groups added: as EGCG has 1 and PGG 5, the concentration of EGCG is the same as that of the scale, but the concentration of PGG is one-fifth that of the scale. The actual concentration of PGG is indicated by the scale at the top of the figure. Different experiments produced a similar pattern but numerically different results, depending on experimental conditions. An estimate of the error can be obtained from the right-hand end of the EGCG data, which are expected to be essentially horizontal.

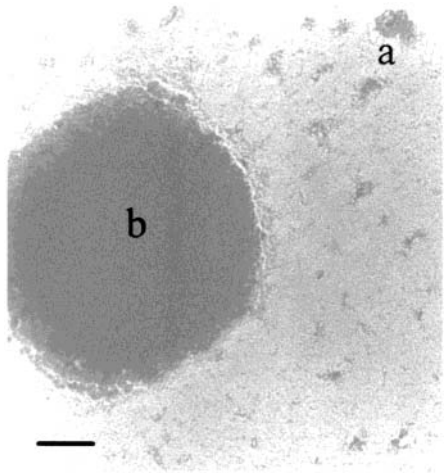

Figure 4. Electron micrograph at a magnification of 104000 of the complex formed by 0.19 mM 19-mer PRP repeat and 0.19 mM EGCG, pH 6.0, at room temperature. The size of the bar is 100 nm. Two particle sizes are evident, with approximate diameters of 80 nm (a) and 500 nm (b).

Electron micrographs of the EGCG/peptide complex (**Figure 4**) show that two classes of particles are formed: a small particle of ~80 nm diameter, with quite diffuse density and irregular shape, and a larger, denser particle of ~500 nm diameter.

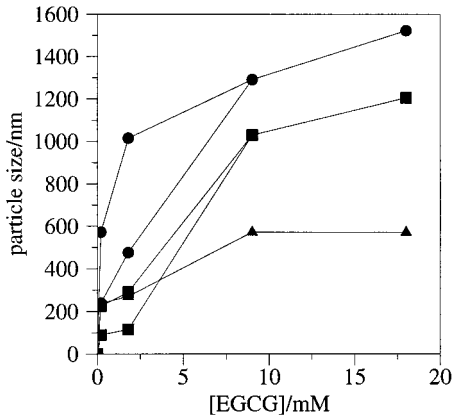

Figure 5. Effect of EGCG concentration and temperature on particle size. All measurements used 0.19 mM 19-mer PRP repeat, pH 6.0, and were made 24 h after preparation of the mixtures. Samples were maintained throughout at the measurement temperature of 17 °C (circles), 36 °C (squares), or 45 °C (triangles).

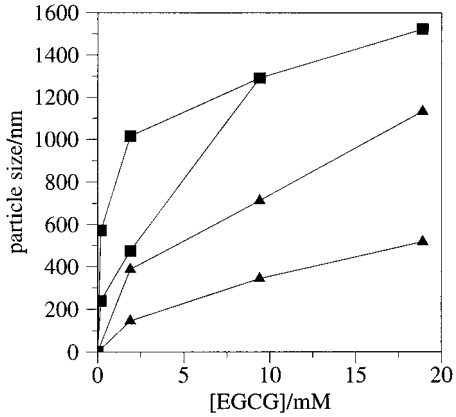

Figure 6. Particle size at increasing EGCG concentration for pH values 3.8 (triangles) and 6.0 (squares). All measurements were made at 27 °C, 24 h after preparation of the mixtures.

Dynamic Laser Light Scattering. Dynamic laser light scattering measures the relaxation rate of particles in a solution that scatter light and, thereby, permits an estimation of their diameter. Measurements were carried out over a wide range of solution conditions. **Figure 5** shows the effect on particle size of increasing EGCG concentration, which not surprisingly is to increase the particle size. However, it is immediately apparent that at lower EGCG concentrations, there are two particle sizes present but that at higher concentrations only the larger particle is seen. (The software package essentially fits the data to the simplest model possible. Thus, it will fit a single species if possible, then it will try two species, and so on. The fact that the data are fitted to two particle sizes therefore does not necessarily imply that only two particle sizes are present. However, the good match between the scattering results and the electron microscopy results suggests that a two-particle model is a good fit to the data.) Increasing the temperature causes the particles to become smaller and also affects the EGCG concentration at which the smaller particles disappear.

More precipitate is visible at higher pH values. Therefore, the effect of pH was also measured and is shown in **Figure 6**. Particle sizes are larger at higher pH (confirmed by other results, not shown, at pH 4.8). As seen for **Figure 5**, there is a bimodal particle size distribution at lower EGCG concentrations.

The sizes of particles seen in these studies fit reasonably well to those observed by electron microscopy. The size of the smaller particle is somewhat larger than that measured in the electron micrographs, but at least some of the difference could be due to the somewhat diffuse and nonspherical nature of the particles, which might tend to make them appear larger in the light scattering experiments than they really are.

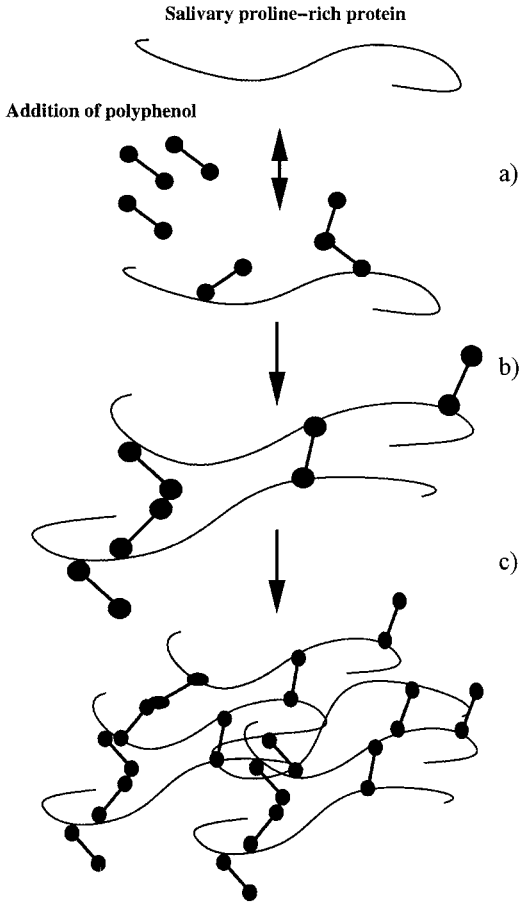

Figure 7. Schematic representation of the stages occurring in binding and precipitation of polyphenols by salivary proline-rich proteins: (a) reversible hydrophobically driven binding of polyphenol, giving a soluble complex; (b) on addition of more polyphenol, two peptides are cross-linked (by at least two polyphenol/protein interactions) and the complex becomes insoluble; (c) further aggregation (phase separation) of the insoluble complexes occurs. The extent of aggregation is determined by surface charge.

DISCUSSION

The interactions between polyphenol and peptide can be divided into three stages (**Figure 7**). Initially, added polyphenol binds to the peptide, and in general several polyphenol molecules can bind to the same peptide. This continues as more polyphenol is added, until the second stage is reached, by which point there is enough polyphenol bound to the peptide to act as a linker between two peptide molecules. The peptide then forms a polyphenol-coated dimer, which starts to precipitate. As it precipitates, more molecules are added, and in the third and final stage, the complex aggregates into either a small particle or a large particle. These stages are now discussed in more detail.

Initial Binding Interaction. The peptides used here were all in an extended or random coil conformation, as indeed they are in the in vivo situation. Polyphenols bind reversibly and relatively weakly at each individual binding site, which may be approximated as 1−2 amino acids long for EGCG and as 5−10 amino acids for the larger PGG molecule. (For the PGG/

bradykinin interaction, the binding site is smaller, most likely because each phenylalanyl side chain presents a larger and more exposed site.) The markedly stronger binding for the 19-mer peptide than for the 7-mer, and the similarity of the affinity at different binding sites, suggest that, particularly for PGG, the polyphenol binds cooperatively at several sites on the peptide, thereby increasing the overall affinity. The binding is largely at exposed hydrophobic and approximately planar side chains, suggesting that it is dominated by stacking of the polyphenolic (and in particular the exposed galloyl) rings against hydrophobic surfaces. Such a conclusion would also be consistent with the order of binding affinity of the polyphenols studied, namely, pentagalloylglucose > tetragalloylglucose > trigalloylglucose ≫ EGCG ≈ ECG (**Tables 1** and **2** and ref *25*), which parallels the number of 1,2-dihydroxyphenyl rings possessed by these molecules, namely, 5, 4, 3, 2, and 2, respectively. A similar relationship was observed in ref *38*. The very small chemical shift changes seen with the histatins suggest that there is little or no binding to the histatins, consistent with the very small amount of visible precipitate using these peptides. However, this result is not consistent with those reported by Bennick and suggests that more work needs to be done in this area.

The results obtained suggest that binding and precipitation are related but not identical, because binding affinities at different pH values were found to be identical, but the amount of visible precipitate, as well as the particle size measured by light scattering, were much greater at higher pH. The solution to this problem comes from the diffusion measurements and from the observations on the particles formed.

The diffusion results show the average diffusion constant for the *soluble* peptide only (because the insoluble peptide complex is NMR-invisible). They show that the diffusion constant decreases steadily (i.e., the aggregate on average increases in molecular weight) until the start of precipitation. After this point the diffusion constant remains essentially unchanged. The change in gradient of the diffusion constant with polyphenol concentration at the onset of precipitation is quite sudden, particularly for EGCG. This implies first that the soluble aggregates do not contain peptide dimers, because otherwise the diffusion constant would continue to decrease markedly, and second that the soluble peptides do not continue to get more and more coated by addition of further polyphenol, but rather that addition of polyphenol beyond a certain point (indicated by the arrows in **Figure 3**) causes them to precipitate out of solution. Thus, the evidence suggests that there is a critical level of coating of the peptide by polyphenol and that when this level is exceeded, the complex precipitates. We therefore turn now to the first precipitated species.

First Precipitated Species. The size of the soluble particle at the onset of precipitation can be estimated from the diffusion experiments (**Figure 3**). Theory shows that for a spherical particle, the diffusion constant (D) is proportional to $1/r$ (where r is the radius of the particle). Assuming a fixed density of the particle, this implies that $D \propto M^{-1/3}$, where M is the mass of the particle. In our case, the particle is unlikely to be spherical due to the elongated nature of the salivary peptide (*10*), and the dependence of D on M will be weaker. As a very crude approximation a dependence of $D \propto M^{-1/2}$ has been assumed. For EGCG, D reduces by 18% before precipitation starts (**Figure 3**). For an initial 19-mer peptide mass of 2200 Da, this implies an increase in mass of ∼50%, or ∼1100 Da. This is therefore consistent with ∼3 EGCG molecules coating each peptide, which would result in an increase in molecular mass of 1374 and clearly be inconsistent with peptide dimers or higher aggregates.

Similarly, the change in the relative diffusion coefficient of the peptide complex with PGG can be used to calculate the approximate mass of this complex at the point of precipitation. The peptide/PGG complex begins to precipitate when the concentration of PGG is ∼1.3 mM (**Figure 3**). At this concentration the diffusion coefficient of the complex is ∼10% lower than that of the uncomplexed peptide. Using the relationship between the diffusion coefficient and the mass of the complex outlined in the previous paragraph, the 10% change in diffusion coefficient equates to a 23% increase in mass. This gives a molecular weight increase of ∼500. Again, this is inconsistent with the formation of a complex including more than one peptide molecule. As the molecular weight of PGG is 1109, these calculations suggest that ∼0.5 of a PGG molecule is bound to each peptide when the complex begins to precipitate.

The number of molecules of both EGCG and PGG bound to the peptide at the onset of precipitation can also be estimated independently using the dissociation constants calculated for each. For EGCG at 3 °C and pH 3.8 the self-association constant (K_a) was measured to be 0.049 mM^{-1} (**Table 2**). Using eq 5 the concentration of monomeric EGCG can be calculated for the EGCG concentration at which precipitation of the peptide/EGCG complex was first observed ($[T]_0 = 11.4$ mM): EGCG is calculated to be ∼50% monomeric at this concentration. Application of eq 6 gives a dimer concentration of 1.66 mM at the onset of precipitation, which when doubled (as there are 2 EGCGs in each dimer) gives 3.3 mM EGCG present as dimers, or ∼30% of the total amount of EGCG. By calculating how many of the 3.1 (**Table 2**) EGCG binding sites on the peptide are occupied and using the ratio of monomers to dimers at the onset of precipitation, an approximation to the total number of EGCG molecules bound to each peptide can be made. The dissociation constant (K_d) for the interaction between EGCG and the proline-rich peptide is 2.4 mM (**Table 2**). The concentration of the proline-rich peptide at the onset of precipitation is 2.3 mM and, as previously stated, the concentration of EGCG is 11.4 mM. Using these two concentrations as $[P]_i$ and $[T]_i$ and substituting them into eq 2 (along with $n = 3.1$ and $K_d = 2.4$ mM), the concentration of bound peptide can be calculated to be 1.7 mM. This is 75% of the total peptide present. It is important here to note that this means that 75% of each of the peptide binding sites is occupied, rather than that 75% of the peptides have EGCG bound. Assuming that all of the binding sites on the peptide have equal affinity (as the isodesmic model for self-association does), then the average number of occupied binding sites should be 0.75 multiplied by n. Therefore, this calculation suggests that ∼2.3 (or roughly 2 of the $n = 3.1$ possible) of the EGCG binding sites are occupied per peptide molecule. Because EGCG is 50% monomeric at 11.4 mM, one of these sites is most probably occupied by an EGCG monomer and the other by a dimer (most likely) or higher aggregate. Although both this and the calculation derived for the diffusion coefficient are very approximate, they are consistent because they both conclude that there are likely to be 3 molecules of EGCG bound to each peptide when the complex begins to become insoluble.

The equivalent binding data have been used to repeat the above calculation for PGG. PGG has a self-association constant of 0.24 mM^{-1} and a peptide dissociation constant of 0.05 mM with 2.2 binding sites per peptide (**Table 2**). At pH 3.8 and 3 °C, PGG was found to precipitate the proline-rich peptide at a

peptide concentration of 3.3 mM and a PGG concentration of 1.3 mM. At 1.3 mM, PGG is calculated to be 64% monomeric and 26% dimeric. Using eq 2 and values of $[P]_i = 3.3$, $[T]_i = 1.3$, $n = 2.2$, and $K_d = 0.05$ mM, the concentration of bound peptide is 0.59 mM or 18% of the total peptide concentration. Multiplying 2.2 by 0.18 suggests that ~0.4 PGG binding sites per peptide are occupied when the complex begins to precipitate. The number of PGG molecules bound to the peptide will be slightly >0.4 due to the oligomerization of the PGG, a finding that is consistent with the value of 0.5 PGG molecules per peptide suggested from the diffusion data.

In summary, these results suggest that the addition of polyphenol to a proline-rich peptide leads to the coating of the peptide, up to a critical point after which precipitation begins. The number of polyphenol molecules required to precipitate the peptide is dependent on the size of the polyphenol and probably more directly on the number of 1,2-dihydroxyphenyl rings that it possesses. In the case of EGCG and PGG, presented above, it is certainly true that the concentration of PGG required to precipitate the peptide is considerably lower than that of EGCG. The calculations above suggest that precipitation of the peptide/EGCG complex starts when there are roughly 3 EGCG molecules (one dimer and one monomer) on each peptide, whereas precipitation of the peptide/PGG complex starts when there is roughly one PGG molecule per peptide pair. It is suggested that the main difference between EGCG and PGG is the greater number of available 1,2-dihydroxyphenyl rings on PGG compared to EGCG (five compared to two). Therefore, these results are consistent with a model in which the role of the polyphenol is to provide a cross-link between two proline-rich peptides and, in particular, one in which there is some element of cooperativity to strengthen the cross-linking interaction. For EGCG the cooperativity comes from the presence of two cross-linking interactions, whereas for PGG it comes from the presence of multiple free 1,2-dihydroxyphenyl rings on the polyphenol. Once a stable cross-linked peptide pair is formed, precipitation can start.

Insoluble Particles. Both the dynamic laser light scattering results and the electron micrographs of the peptide/EGCG complex suggest that at low ratios of polyphenol to peptide there are two species of insoluble particle present, with approximate diameters of 80 and 500 nm. From the size of the 19-mer extended peptide (~7 nm) and the diffuse irregular appearance of the smaller particle compared to the denser and more spherical appearance of the larger one, this suggests that the smaller particle may consist of ~20 peptide dimers in a rather open arrangement. However, the larger particle is probably denser and contains at least 20 times more molecules. The distribution of particle sizes depends on the concentration of polyphenols, on temperature, and on pH. However, the binding affinities are the same at the different pH values studied, implying that the change in particle size does not result from a change in peptide/polyphenol affinity. Rather, these observations follow the behavior expected for a colloidal suspension, in which small particles are prevented from aggregating together to form larger particles by their surface charges. EGCG itself has a pK_a of ~8.8, suggesting that the pH dependence of aggregation in the range 3.8−6.0 is unlikely to be due to the polyphenol and is more likely to be due to the C-terminal carboxyl group, with a pK_a of ~3.1. The arginine side chain will make the peptide net positively charged at all pH values studied, but clearly the net charge will be less at higher pH and an aggregate of several hundred peptide molecules will be more stable when its net charge is lower. Thus, although the initial binding of polyphenol to peptide and the dimerization of the peptide to form the first insoluble particle is essentially a hydrophobically driven interaction, the eventual size of the insoluble particle is most likely determined by surface charge effects.

At this point it is helpful to consider further the meaning of the word "insoluble". Formally, a solute becomes insoluble when the free energy for the solvated species becomes higher than the free energy for the unsolvated species. However, this simple (and almost trivial) definition hides a complex set of ideas. For example, precipitation (which here is used as an equivalent term to "loss of solubility") is not usually a unimolecular process: indeed, it is not clear whether it is valid to think of a single molecule as "becoming insoluble" by itself. It is more useful to discuss precipitation in terms of phase changes. When the chemical potential of a solution changes (for example, by changing the temperature or composition), it can pass through a phase boundary, such that two previously miscible substances (i.e., solute and solvent) become immiscible. The process of phase separation can occur in two main ways (*39*). The more common way has an associated activation energy and therefore involves nucleation and growth. The alternative way has no activation energy barrier and happens spontaneously as soon as a phase boundary is passed. It has been particularly well studied in branches of material science such as metal alloy cooling, where the phase separation is referred to as spinodal decomposition. In the case studied here, there is no evidence for nucleation (as seen by the observation that there are two distinct particle sizes, with essentially no intermediates, and that formation of the insoluble aggregate begins immediately on mixing), and it is suggested that the formation of insoluble particles is best described as a phase separation or as a spinodal decomposition. This spontaneous spinodal phase separation is a phenomenon that has previously been observed when the polyphenols present in black tea complex to form large aggregates during the process of tea creaming as tea cools (*40*).

Conclusions. The way in which polyphenols bind to the proline-rich peptide can be divided into three distinct phases (**Figure 7**). The initial interaction is the complexation of the peptide by molecules of polyphenol to form soluble aggregates. The aggregates are single peptide molecules with polyphenols bound by the hydrophobic face of the aromatic rings to the pyrrolidine ring of the proline residues. The second stage requires the recruitment of a second polyphenol-coated peptide molecule, driven by cooperative weak intermolecular bridging interactions carried out by the polyphenol, leading to a doubling in the size of the complex, which renders the complex insoluble. In the third stage, a small number of these peptide dimers aggregate together until the charge repulsion between them balances out the favorable interaction energy. Finally, the spontaneous aggregation of these insoluble aggregates into larger complexes leads to the bimodal distribution of particle sizes seen in the laser light scattering experiments and visualized by the electron micrographs, in what is most simply seen as a phase separation process.

ABBREVIATIONS USED

ECG, epicatechin gallate; EGCG, epigallocatechin gallate; PGG, pentagalloyl glucose; tetraGG, tetragalloylglucose; triGG, trigalloylglucose.

ACKNOWLEDGMENT

We thank D. Jones and Dr. W. Frith (Unilever) for assistance with the light scattering experiments and John Procter (University of Sheffield) for carrying out the electron microscopy.

Supporting Information Available: Chemical shift assignments for the N-terminal acidic proline-rich peptide, and average (± standard deviation) chemical shift changes of each residue of the N-terminal acidic proline-rich peptide on addition of 5 molar equiv of propyl gallate. This material is available free of charge via the Internet at http://pubs.acs.org.

LITERATURE CITED

(1) Haslam, E. *Plant Polyphenols*; Cambridge University Press: Cambridge, U.K., 1989.

(2) Bate-Smith, E. C. Haem analysis of tannins—the concept of relative astringency. *Phytochemistry* **1973**, *12*, 907−912.

(3) Kallithraka, S.; Bakker, J.; Clifford, M. N. Evidence that salivary proteins are involved in astringency. *J. Sens. Stud.* **1998**, *13*, 29−43.

(4) Kauffman, D. L.; Keller, P. J. The basic proline-rich proteins in human parotid saliva from a single subject. *Arch. Oral Biol.* **1979**, *24*, 249−256.

(5) Bennick, A. Salivary proline-rich proteins. *Mol. Cell. Biochem.* **1982**, *45*, 83−99.

(6) Bennick, A.; McLaughlin, A. C.; Grey, A. A.; Madapallimattam, G. The location and nature of calcium-binding sites in salivary acidic proline-rich phosphoproteins. *J. Biol. Chem.* **1981**, *256*, 4741−4746.

(7) Hatton, M. N.; Loomis, R. E.; Levine, M. J.; Tabak, L. A. Masticatory lubrication. The role of carbohydrate in the lubricating property of a salivary protein albumin complex. *Biochem. J.* **1985**, *230*, 817−820.

(8) Hagerman, A. E.; Butler, L. G. The specificity of the proanthocyanidin-protein interaction. *J. Biol. Chem.* **1981**, *256*, 4494−4497.

(9) Bennick, A. Structural and genetic aspects of proline-rich proteins. *J. Dent. Res.* **1987**, *66*, 457−461.

(10) Murray, N. J.; Williamson, M. P. Conformational study of a proline-rich protein repeat sequence. *Eur. J. Biochem.* **1994**, *219*, 915−921.

(11) Mehansho, H.; Butler, L. G.; Carlson, D. M. Dietary tanins and salivary proline-rich proteins: Interactions, induction and defense mechanisms. *Annu. Rev. Nutr.* **1987**, *7*, 423−440.

(12) Warner, T. F.; Azen, E. A. Tannins, salivary proline-rich proteins and oesophageal cancer. *Med. Hypoth.* **1988**, *26*, 99−102.

(13) Lu, Y.; Bennick, A. Interaction of tannin with human salivary proline-rich proteins. *Arch. Oral Biol.* **1998**, *43*, 717−728.

(14) Mole, S.; Butler, L. G.; Iason, G. Defense against dietary tannin in herbivores: A survey for proline-rich salivary proteins in mammals. *Biochem. Syst. Ecol.* **1990**, *18*, 287−293.

(15) Armitage, R.; Bayliss, G. S.; Gramshaw, J. W.; Haslam, E.; Haworth, R. D.; Jones, K.; Rogers, H. J.; Searle, T. Gallotannins. Part III. The constitution of chinese, turkish, sumach and tara tannins. *J. Chem. Soc.* **1961**, 1842−1853.

(16) Schmidt, O. T.; Demmler, K.; Bittermann, H.; Stephan, P. Über natürliche Gerbstoffe XXVII. Neochebulinsäure und 1.3.6-Trigalloylglucose. *Liebigs Ann. Chem.* **1957**, *609*, 192−199.

(17) Thompson, R. S.; Jacques, D.; Haslam, E.; Tanner, R. J. N. Plant proanthocyanins. Part 1. Introduction; the isolation, structure and distribution in nature of plant proanthocyanidins. *J. Chem. Soc., Perkin Trans. 1* **1972**, 1387−1399.

(18) Layfield, R.; Bannister, A. J.; Pierce, E. J.; McDonald, C. J. cDNA clones for mouse parotid proline-rich proteins—mRNA regulation by isoprenaline and the nucleotide sequence of proline-rich protein cDNA MP5. *Eur. J. Biochem.* **1992**, *204*, 591−597.

(19) Levine, M. J.; Keller, P. J. The isolation of some basic proline-rich proteins from human parotid saliva. *Arch. Oral Biol.* **1977**, *22*, 37−41.

(20) Kauffman, D. L.; Wong, R.; Bennick, A.; Keller, P. J. Basic proline-rich proteins from human saliva: Complete covalent structure of protein IB-9 and partial structure of protein IB-6, members of a polymorphic pair. *Biochemistry* **1982**, *21*, 6558−6562.

(21) Kauffman, D. L.; Hoffman, T.; Bennick, A.; Keller, P. J. Basic proline-rich proteins from human parotid saliva: Complete covalent structures of proteins IB-1 and IB-6. *Biochemistry* **1986**, *25*, 2387−2392.

(22) Kauffman, D. L.; Bennick, A.; Blum, M.; Keller, P. J. Basic proline-rich proteins from human parotid saliva: Relationships of the covalent structures of 10 proteins from a single individual. *Biochemistry* **1991**, *30*, 3351−3356.

(23) Curby, W. A. Device for collection of human parotid saliva. *J. Lab. Clin. Med.* **1953**, *41*, 493−496.

(24) Charlton, A. J.; Baxter, N. J.; Lilley, T. H.; Haslam, E.; McDonald, C. J.; Williamson, M. P. Tannin interactions with a full-length human salivary proline-rich protein display a stronger affinity than with single proline-rich repeats. *FEBS Lett.* **1996**, *382*, 289−292.

(25) Baxter, N. J.; Williamson, M. P.; Lilley, T. H.; Haslam, E. Stacking interactions between caffeine and methyl gallate. *J. Chem. Soc., Faraday Trans.* **1996**, *92*, 231−234.

(26) Baxter, N. J.; Lilley, T. H.; Haslam, E.; Williamson, M. P. Multiple interactions between polyphenols and a salivary proline-rich protein repeat result in complexation and precipitation. *Biochemistry* **1997**, *36*, 5566−5577.

(27) Altieri, A. S.; Hinton, D. P.; Byrd, R. A. Association of biomolecular systems *via* pulsed field gradient NMR self-diffusion measurements. *J. Am. Chem. Soc.* **1995**, *117*, 7566−7567.

(28) Thormählen, J. S.; Grigull, U. Refractive index of water and its dependence on wavelength, temperature and density. *J. Phys. Chem. Ref. Data* **1985**, *14*, 933−945.

(29) Wüthrich, K. *NMR of Proteins and Nucleic Acids*; Wiley: New York, 1986.

(30) Murray, N. J. NMR Studies of Salivary Proline-Rich Proteins and Tannins; Ph.D. Thesis, University of Sheffield, Sheffield, U.K., 1994.

(31) Khan, M. L. UV and NMR Studies of Tannin Complexation; Ph.D. Thesis, University of Sheffield, Sheffield, U.K., 1996.

(32) Charlton, A. J. Study of the Interaction between Salivary Proline-Rich Proteins and Plant Polyphenols; Ph.D. Thesis, University of Sheffield, Sheffield, U.K., 2000.

(33) Davis, A. L.; Cai, Y.; Davies, A. P.; Lewis, J. R. ^{1}H and ^{13}C NMR assignments of some green tea polyphenols. *Magn. Reson. Chem.* **1996**, *34*, 887−890.

(34) Murray, N. J.; Williamson, M. P.; Lilley, T. H.; Haslam, E. Study of a salivary proline-rich protein and a polyphenol by ^{1}H-NMR spectroscopy. *Eur. J. Biochem.* **1994**, *219*, 923−935.

(35) Yan, Q.; Bennick, A. Identification of histatins as tannin-binding proteins in human saliva. *Biochem. J.* **1995**, *311*, 341−347.

(36) Naurato, N.; Wong, P.; Lu, Y.; Wroblewski, K.; Bennick, A. Interaction of tannin with human salivary histatin. *J. Agric. Food Chem.* **1999**, *47*, 2229−2234.

(37) Wroblewski, K.; Muhandiram, R.; Chakrabartty, A.; Bennick, A. The molecular interaction of human salivary histatins with polyphenolic compounds. *Eir. J. Biochem.* **2001**, *268*, 4384−4397.

(38) Bacon, J. R.; Rhodes, M. J. C. Development of a competition assay for the evaluation of the binding of human parotid salivary proteins to dietary complex polyphenols and tannins using a peroxidase-labeled tannin. *J. Agric. Food Chem.* **1998**, *46*, 5083−5088.

(39) Porter, D. A.; Easterling, K. E. *Phase Transformation in Metals and Alloys*; Van Nostrand Reinhold: Wokingham, U.K., 1981; pp 308−315.

(40) Penders, M. H. G. M.; Jones, D. J.; Needham, D.; Pelan, E. G.; Underwood, D. R.; Scollard, D. J. P.; Davies, A. P. Kinetics and thermodynamics of tea cream formation: A colloidal approach. *Prog. Colloid Polym. Sci.* **1998**, *110*, 163−170.

Received for review July 11, 2001. Revised manuscript received November 23, 2001. Accepted December 18, 2001.

JF010897Z